ARTICLE
Journal of Cellular Biochemistry 115:2089–2102 (2014)

Journal of Cellular Biochemistry

Osteogenic Cell Cultures Cannot Utilize Exogenous Sources of Synthetic Polyphosphate for Mineralization

Marianne B. Ariganello,[1] Sidney Omelon,[2] Fabio Variola,[2] Rima M. Wazen,[1] Pierre Moffatt,[3,4] and Antonio Nanci[1,5]*

[1]*Department of Stomatology, Faculty of Dentistry, Université de Montréal, P.O. Box 6128 Station Centre-Ville, Montréal Québec, Canada H3C 3J7*

[2]*Faculty of Engineering, University of Ottawa, Colonel By Hall 161 Louis Pasteur, Ottawa, Ontario, Canada K1N 6N5*

[3]*Genetics Unit, Shriners Hospital for Children, 1529 Cedar Ave. Montréal, Québec, Canada H3G 1A6*

[4]*Department of Human Genetics, McGill University, Stewart Biology Building, 1205 Dr. Penfield Ave. Montréal, Québec, Canada H3A 2T5*

[5]*Department of Biochemistry and Molecular Medicine, Université de Montréal, Montréal, Québec, Canada*

ABSTRACT

Phosphate is critical for mineralization and deficiencies in the regulation of free phosphate lead to disease. Inorganic polyphosphates (polyPs) may represent a physiological source of phosphate because they can be hydrolyzed by biological phosphatases. To investigate whether exogenous polyP could be utilized for mineral formation, mineralization was evaluated in two osteogenic cell lines, Saos-2 and MC3T3, expressing different levels of tissue non-specific alkaline phosphatase (tnALP). The role of tnALP was further explored by lentiviral-mediated overexpression in MC3T3 cells. When cells were cultured in the presence of three different phosphate sources, there was a strong mineralization response with β-glycerophosphate (βGP) and orthophosphate (Pi) but none of the cultures sustained mineralization in the presence of polyP (neither chain length 17-Pi nor 42-Pi). Even in the presence of mineralizing levels of phosphate, low concentrations of polyP (50 μM) were sufficient to inhibit mineral formation. Energy-dispersive X-ray spectroscopy confirmed the presence of apatite-like mineral deposits in MC3T3 cultures supplemented with βGP, but not in those with polyP. While von Kossa staining was consistent with the presence or absence of mineral, an unusual Alizarin staining was obtained in polyP-treated MC3T3 cultures. This staining pattern combined with low Ca:P ratios suggests the persistence of Ca-polyP complexes, even with high residual ALP activity. In conclusion, under standard culture conditions, exogenous polyP does not promote mineral deposition. This is not due to a lack of active ALP, and unless conditions that favor significant processing of polyP are achieved, its mineral inhibitory capacity predominates. J. Cell. Biochem. 115: 2089–2102, 2014.

KEY WORDS: POLYPHOSPHATE; PHOSPHATE; MINERALIZATION; OSTEOBLASTS; ALKALINE PHOSPHATASE; LENTIVIRAL VECTOR; ALIZARIN RED

Negatively-charged polymers of phosphate (polyphosphates, polyPs) are found within body fluids (such as synovia and blood) as well as in a variety of mammalian cells (platelets, mononuclear cells, fibroblasts, and osteoblasts) [Kumble and Kornberg, 1995; Müller et al., 2009]. While polyPs (historically known as Graham's salts or condensed phosphates) have been detected within the nuclei, mitochondria and plasma membrane of mammalian cells, other cellular distributions cannot be excluded [Leyhausen et al., 1998; Kornberg et al., 1999]. A variety of roles for intracellular polyPs have been proposed, including acting as a protein chaperone [Gray et al., 2014], involvement in mitochondrial function and membrane depolarization [Abramov et al., 2007], cell energy metabolism [Pavlov et al., 2010], signal transmission in the brain [Holmström et al., 2013], normal ion channel activity

Abbreviations: AA, ascorbic acid; ALP, alkaline phosphatase; βGP, β-glycerophosphate; BSE, backscattered electron imaging; EDS, energy dispersive X-ray spectroscopy; FBS, Fetal Bovine Serum; FGF, Fibroblast Growth Factor; HEK, human embryonic kidney; LV, lentiviral vector; MEM, modified essential media; PBS, phosphate-buffered saline; Pi, orthophosphate; pNPP, p-nitrophenylphosphate; polyP, polyphosphate; PPK, polyphosphate kinase; PPX, exopolyphosphatases; SEI, secondary electron imaging; SEM, scanning electron microscopy; tnALP, tissue non-specific alkaline phosphatase; Vtc4, vacuolar transporter chaperone 4; VSVG, vesicular stomatitis virus G.

*Correspondence to: Antonio Nanci, Department of Stomatology, Faculty of Dentistry, Université de Montréal 2900 Edouard Montpetit Blvd. Pavillon Roger-Gaudry, Montréal Québec, Canada, H3C 3J7.
E-mail: antonio.nanci@umontreal.ca

Manuscript Received: 2 November 2013; Manuscript Accepted: 10 July 2014
Accepted manuscript online in Wiley Online Library (wileyonlinelibrary.com): 16 July 2014
DOI 10.1002/jcb.24886 • © 2014 Wiley Periodicals, Inc.

[Zakharian et al., 2009], blood coagulation [Smith et al., 2006], and inflammation [Müller et al., 2009].

In their most basic form, these long phosphate chains are biochemically generated by the polymerisation of phosphate. The exact synthesizing enzymes and processes have yet to be elucidated in most mammalian cells, since the phosphate-polymerizing enzymes identified in bacteria (polyphosphate kinase, PPK) and yeast (vacuolar transporter chaperone 4, Vtc4), are not common to mammalian cells [Kornberg et al., 1999; Azevedo and Saiardi, 2014]. The biological formation of polyP in vivo from an inorganic phosphate pool reduces the local, free inorganic phosphate concentration. It also retains a bioavailable bank of phosphorus that is released as orthophosphate (Pi) following enzymatic cleavage from polyP. Mammalian cell extracts contain constituents that have the biochemical capacity to cleave synthetic polyP chains, although the particular enzyme identities are still under investigation [Kumble and Kornberg, 1996; Leyhausen et al., 1998; Kohn et al., 2012]. Tissue non-specific alkaline phosphatase (tnALP) is an example of a mammalian enzyme that has been shown to have the biochemical capacity to degrade polyP (i.e., in laboratory settings under conditions of basic pH and in the presence of Mg^{2+}) [Omelon et al., 2009; Hoac et al., 2013], although its biological efficacy of cleaving Pi from polyP in vitro (and in vivo) has not been definitively established. TnALP is a membrane-bound enzyme that is commonly associated with skeletal mineralization and cleavage of pyrophosphate into two Pi ions [Millán, 2006]. Given the requirement of phosphorus in numerous cell processes, the simple biochemical mechanism for phosphorus banking through a polyP species is ideal. As large polyanions, polyPs have a great affinity for calcium and other divalent cations [Van Wazer and Campanella, 1950] and can produce an amorphous and charge-neutral $[Ca(PO_3)_2]_n$ complex. This chelation mechanism additionally reduces the local free calcium ion concentration. The chemical composition of the Ca-polyP complex is a function of the polyP chain length, but the Ca:P ratio of these complexes is always less than 1.0 [Landis and Glimcher, 1978]. The neutral complex represents a concentrated store of bioavailable Ca^{2+} and PO_4^{3-}, which could be used for apatite mineralization. The theory of polyPs as an intrinsic source for Ca^{2+} and Pi for mineralization is strengthened by the observation that osteoblast cells contain higher amounts of polyP compared to soft tissue cells [Leyhausen et al., 1998].

The objective of this study was to determine whether synthetic polyP could be used as an exogenous source of Pi for mineralization in cell culture, as compared to the in vitro standard β-glycerophosphate (βGP). Since tnALP is implicated in the cleavage of phosphorous–oxygen–phosphorous (P–O–P) bonds in vitro and in vivo, we hypothesized that polyP could be similarly broken down to generate free Pi, which could be used in the formation of apatite mineral. To understand the role(s) that tnALP may play in the metabolism of exogenous polyP, we studied two different osteogenic cell lines that express different endogenous levels of tnALP, that is, human Saos-2 cells and mouse MC3T3 cells [Murray et al., 1987; Beck et al., 1998]. In addition, we used a lentiviral vector to enhance the tnALP expression in MC3T3 cells. Our results demonstrated that exogenous polyP does not play a major role in initiating mineral deposition in cell cultures, and that tnALP, irrespective of its level of expression, cannot achieve complete processing of the polyP to sustain mineralization under the culture conditions used. A better understanding of polyP biochemistry could lead to the therapeutic use of polyP for mineralization disorders, and aid in understanding the physiological significance of intracellular polyP, particularly in osteogenic cells.

MATERIALS AND METHODS

CELL CULTURE SUPPLIES

Glass microscope coverslips used for cell culture were obtained from ThermoFisher Scientific (Whitby, ON, Canada). All other products were obtained from Life Technologies (Mississauga, ON, Canada) unless otherwise specified.

POLYPHOSPHATE SOURCES

Two sources of polyP obtained from Sigma–Aldrich (Oakville, ON, Canada) were tested in this study: Type 45 sodium phosphate glass with certified average phosphate chain length of 42 (polyP42, "longer chain") and sodium hexametaphosphate with certified average phosphate chain length of 17 (polyP17, "shorter chain"). The concentration of polyP is reported either as moles of polymer chain or as moles of Pi equivalents (see Table I). The concentration of polyP used in each experiment was selected so that all phosphate sources tested provided an equivalent concentration of Pi in the media, with Pi-concentration being dependent on the cell type (see below).

CELL CULTURE

Saos-2 osteosarcoma cells (ATCC, Manassas, VA, USA) were cultured in Dulbecco's modified essential media (D-MEM) containing 10% fetal bovine serum (FBS) and trypsinized using 0.25% trypsin–EDTA. For mineralization assays, cells were seeded at a density of 7900/cm^2 in either 12- or 24-well plates (or on coverslips for microscopy analysis) and allowed to grow to confluence for 96 h at 37 °C/5% CO_2 in a humidified incubator. Cells were subsequently treated with mineralizing medium consisting of 50 μM ascorbic acid (AA) combined with a phosphate source. Specifically either 5 mM βGP, 5 mM Pi (from a neutral pH sodium phosphate solution), 412 μM polyP17 (equivalent to 7 mM inorganic Pi) or a range of polyP42 concentrations (from 10–500 μM polyP42) was added as the phosphate source. The respective mineralizing medium was replaced every 2 days or 4 days during the culture period. In some studies, the

TABLE I. Polyphosphate Chain Lengths and Concentrations

Name	Average chain length	Average Pi equivalents*
Type 45 sodium phosphate glass	42 phosphate monomers $\sim(Na\text{-}PO_3)_{42}$	1 mol of polyP42 = 42 molar equivalents of Pi
Sodium hexametaphosphate	17 phosphate monomers $\sim(Na\text{-}PO_3)_{17}$	1 mol of PolyP17 = 17 molar equivalents of Pi

*assuming complete degradation of the polymer into its free orthophosphate (Pi) monomer.

media was supplemented with 3.3 mM Pi to match the baseline concentration found in McCoy's media used in previous polyP studies with Saos-2 cells. Additionally, where noted, dissolved polyP was mixed with calcium chloride solutions (at a ratio of 2:1 (moles of polyphosphate polymer: mole of Ca^{2+}) as described in previous studies [Müller et al., 2011]. These resulting calcium–polyP complexes were formed in aqueous solutions prior to adding them to cell culture media. During cell culture, cells were observed with an inverted microscope (Carl Zeiss, Axio Observer Z1, Jena, Germany).

MC3T3 (E1, subclone 4) pre-osteoblast cells (ATCC) were cultured in αMEM with 10% FBS and trypsinized when sub-confluent using 0.25% trypsin–EDTA. For mineralization assays, cells were seeded at a density of 13000/cm^2 in either 6- or 12-well plates (or on coverslips) and allowed to grow to confluence for 72 h at 37 °C/5% CO_2 in a humidified incubator. Cells were treated with mineralizing media consisting of 50 μg/mL AA combined with either 3 mM βGP, 3 mM Pi, 294 μM polyP17, or 119 μM polyP42 (both equivalent to 5 mM inorganic Pi). Mineralizing medium was replaced every 4 days for either 21 days or 28 days.

LENTIVIRUS INFECTION

A five-plasmid transfection system was used to generate a lentiviral vector (LV) for rat tnALP transgene expression [Wazen et al., 2006]. The tnALP cDNA was amplified by RT-PCR on total RNA extracted from rat tibia using forward 5′-gggtacaccatgatcttgcc-3′ and reverse 5′-cctcagaacagggtgcgtag-3′ primers. The 1586bp fragment covered the entire coding sequence of rat tnALP, matching nucleotides 144–1729 of GenBank clone J0572. The lentivirus was pseudotyped with vesicular stomatitis virus G (VSVG) glycoprotein, packaged using human embryonic kidney (HEK) 293 cells and concentrated by ultracentrifugation. MC3T3 cells were infected with the lentivirus in the presence of 8 μg/mL polybrene overnight, media was exchanged and cells were grown to sub-confluence and then passaged. LV-tnALP overexpression was confirmed microscopically for every cell passage and experiment using Fast Blue ALP and/or spectrophotometrically using a *p*-nitrophenyl phosphate (pNPP) assay (see below). Control cells were exposed to an identical concentration of polybrene without virus and similarly passaged. Both infected and control cells were plated at the same density as above (13000/cm^2) and treated with mineralizing medium upon reaching confluence. Mineralizing medium was replaced every 4 days.

ALP ACTIVITY: pNPP ASSAY AND FAST BLUE ALP STAIN

For evaluation of ALP activity using the pNPP assay, a 4 mg/mL pNPP solution was prepared in alkaline buffer (Sigma A9226, pH 10.3, containing 2-amino-2-methylpropanol) with a final concentration of 10 mM $MgCl_2$. After 24 h of culture in 24-well-plates, the supernatant was aspirated, and 125 uL of the pNPP solution was added to each well. Following an incubation of 10 min at 37 °C, the reaction was stopped with an equivalent volume of 0.5 M NaOH and the absorbance was read at 405 nm. For Fast Blue ALP staining, cells were cultured on coverslips for 24 h, fixed in 70% ethanol or 4% paraformaldehyde in 0.1 M phosphate buffer for at least 1 h, then permeabilized in 0.1 M phosphate buffer containing 0.2% Tween for 10 min. Cells were stained with ALP Fast Blue (Sigma B5655, pH 9.5) in the dark for 10 min. Stain development was arrested by rinsing 3x with 55 °C phosphate-buffered saline (PBS, pH 8.0). Cells were then incubated with 0.9% (w/V) neutral red in 18 mM acetic acid for 10 min. The coverslip was mounted onto a glass slide and analyzed microscopically using an upright microscope (Carl Zeiss, Axio Imager M2).

ALIZARIN RED AND VON KOSSA STAINING

At the end of the mineralization period, cells were fixed in 70% ethanol and then stained with 2% (w/V) Alizarin red solution (pH = 4.1–4.3) for 10 min, rinsed 5x in dH_2O followed by 1x PBS (pH 7.4), then imaged [Puchtler et al., 1969]. For quantitative measurements, wells were extracted with 10% cetylpyridinium chloride and absorbance read at 405 nm [Stanford et al., 1995]. For von Kossa staining, after fixation in ethanol, cells were incubated with 2% silver nitrate (w/V) and exposed to UV light for 10 min, the stain was fixed with sodium thiosulfate [Meloan and Puchtler, 1985].

PHOSPHATE CONCENTRATION IN MC3T3 SUPERNATANTS

At the end of the mineralization period, the supernatants from MC3T3 were collected and frozen for future phosphate analysis. The supernatants were analyzed using PhosphoWorks™ (AAT Bioquest, Sunnyvale, CA, USA) as per manufacturer's direction; briefly, supernatants were diluted in dH_2O then combined with the phosphate sensor prior to reading fluorescence (Ex: 540 nm, Em: 590). Potassium phosphate (KH_2PO_4) was used to generate a standard curve.

SCANNING ELECTRON MICROSCOPY (SEM) AND ENERGY DISPERSIVE X-RAY SPECTROSCOPY (EDS)

At the end of the mineralization period, cells were fixed in 2.5% glutaraldehyde (EMS, Hatfield, PA, USA) in PBS (pH 7.4), dehydrated in increasing ethanol concentrations and critical point dried. Samples were then carbon-coated and imaged in a JEOL JSM-7400F or JEOL JSM-7100FT field emission electron microscope. Secondary electron imaging (SEI) was used to obtain structural information, backscattered electron imaging (BSE) provided atomic compositional contrast and EDS provided elemental composition. EDS was performed on the 7100FT, which was equipped with Oxford Instruments X-Max 50 mm^2 SDD detector and Aztec acquisition and analysis software. The data was collected at 10 kV and each map was acquired for 10 min.

STATISTICAL ANALYSIS

Data is presented as average ± standard error of the mean. Alizarin red solubilization data and phosphate concentrations were analyzed using a one-way ANOVA at an overall significance level of 0.05, Bonferroni-adjusted for multiple comparisons. Tukey post-hoc tests were used to identify differences between groups. All statistical analyses were carried out using JMP software (SAS, version 9.0.1).

RESULTS

TREATMENT OF Saos-2 CELLS WITH UNADULTERATED LONG-CHAIN polyPs

Our objective was to determine whether synthetic, exogenous polyP could be used as an extracellular source of Pi, as compared to the in vitro standard, βGP. When Saos-2 cells were cultured for 4 days in

the presence of βGP, deposits were observed with an inverted light microscope and these were further identified as containing both phosphate (positive von Kossa staining, Fig. 1A) and calcium (positive Alizarin red staining, Fig. 1B). However, when Saos-2 cells were cultured in the presence of either 50 μM or 100 μM polyP42 (corresponding to 2.1 mM Pi equivalents or 4.2 mM Pi equivalents), no mineral deposits were detected by light microscopy, and both von Kossa and Alizarin red staining were negative (Figs. 1A and B). At a

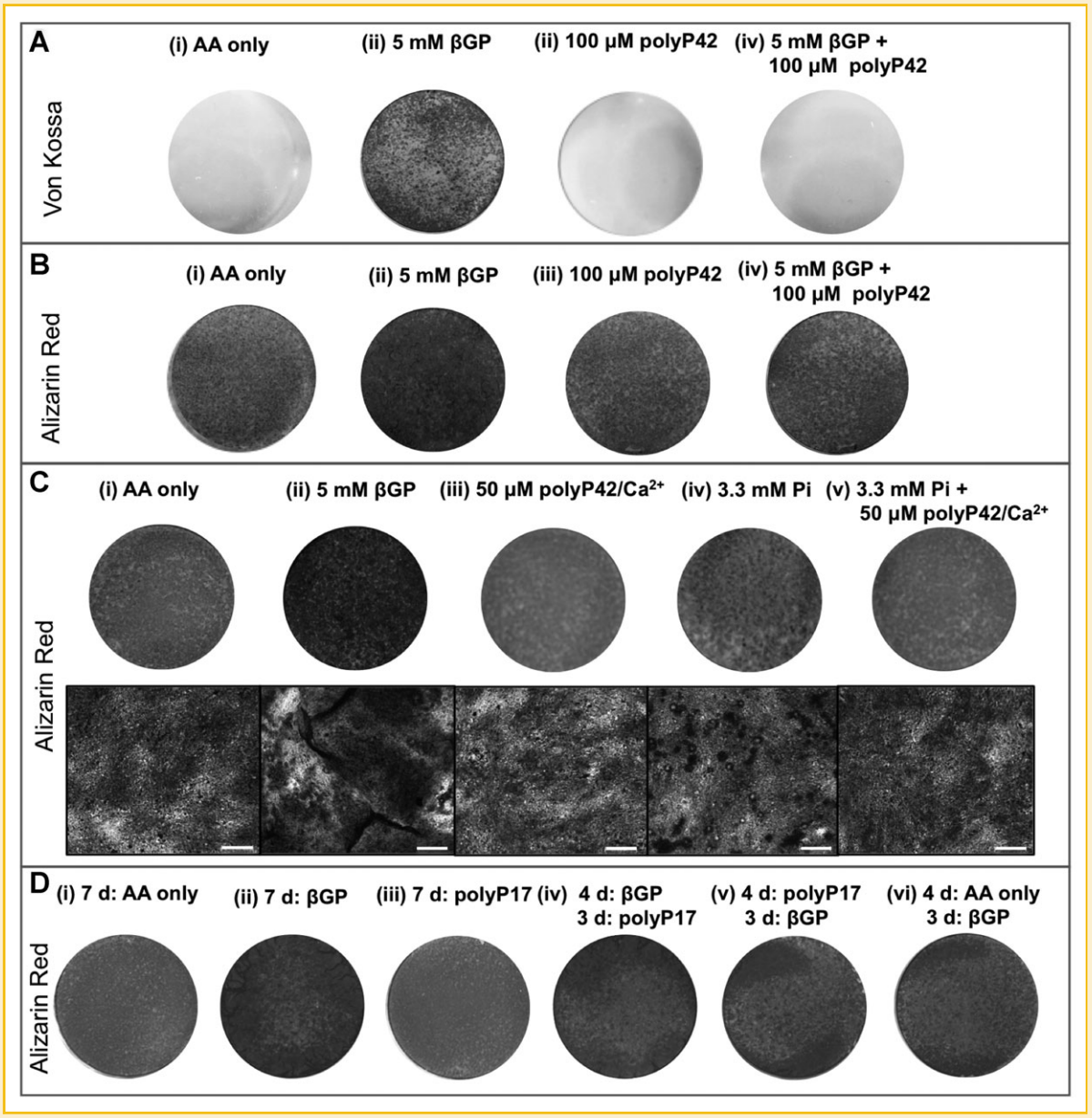

Fig. 1. PolyP cannot be utilized to generate mineral deposition in Saos-2 cultures. Media changed every 2 days during a 4 days mineralization period (A,B). Media changed every 4 days during a 6 days (C) or 7 days (D) mineralization period. In contrast to the standard phosphate source, βGP (A-ii), Saos-2 cells were unable to utilize long chain polyP42 to form mineral deposits (A-iii). This was demonstrated with a negative von Kossa staining for phosphate (A-iii) and negative Alizarin red staining for calcium (B-iii). As was shown in previous studies, when cells are incubated with both βGP and polyP42 (A-iv, B-iv), mineral deposits did not form. Cells incubated in the presence of a high concentration of polyP42 (500 μM) do not survive the 4 days mineralization period (not shown). When polyP42 was complexed with calcium (C-iii), to compensate for any polyP-related chelation effects, or cultured in the presence of high background levels of phosphate (C-v), mineralization was not induced. The small amount of mineralization resulting from a higher baseline concentration of Pi (C-iv) was lost when polyP42 was added to the culture (C-v). High magnification images are included to highlight the mineralization observed in the presence of 3.3 mM Pi (C-iv) and the absence of any visible mineralization, even at the microscopic level, when polyP42 is added to the culture (C-v). Scale bar = 200 μm. The lack of mineralization in the presence of polyP is unaffected by polymer chain length: Saos-2 cells were unable to utilize a shorter chain, polyP17, as a phosphate source, even within an extended mineralization period (D-iii). As well, any inhibition resulting from the presence of polyP17 was not permanent; once the polyP17 was removed, cells were able to mineralize in the presence of βGP (D-v) to the same degree as previously untreated cells (D-vi). Furthermore, even after mineral deposition had begun, subsequent addition of polyP17 did not induce any further mineral deposition (D-iv).

higher concentration of polyP42 (500 μM), cells detached from the culture plate (data not shown). Due to this adverse effect, further studies focused on using concentrations lower than 500 μM polyP.

TREATMENT OF Saos-2 CELLS WITH LONG CHAIN polyP COMPLEXED WITH CALCIUM

To test whether chelation of calcium affected the capacity of exogenous polyP42 to induce mineralization, calcium chloride was combined with polyP42 prior to treatment. Despite the addition of calcium, polyP42-treated cells were still incapable of inducing mineralization after 6 days (Fig. 1C). When a higher complex ratio was used (e.g., 2 mole of Pi equivalents: 1 mole of Ca^{2+}) as described by Wang et al. (2012) no mineralization was detected (data not shown), indicating that the presence of calcium did not sufficiently alter polyP depolymerisation to generate Pi for apatite mineralization.

TREATMENT OF Saos-2 CELLS WITH polyP IN COMBINATION WITH AN ADDITIONAL PHOSPHATE SOURCE

When cells were cultured in the presence of both βGP and polyP42, mineralization was not detected (Figs. 1A and B). Similarly, when cells were cultured in media supplemented with polyP42; and 3.3 mM Pi, mineralization was not observed (Fig. 1C). These results suggest that in both cases, polyP42 prevented mineralization even in the presence of sufficient free phosphate.

TREATMENT OF Saos-2 CELLS WITH SHORTER CHAIN polyPs AND INCREASED DURATION OF EXPOSURE

In order to mimic the non-stagnant nature of fluid flow in the body, mineralization media is typically changed every 2 days, a procedure that periodically replenishes the media with intact, long chain polyP. The absence of mineralization after polyP treatment could therefore be a result of incomplete degradation of the long-chain polymer into free Pi. To test this hypothesis, two experiments were performed: (1) the polyP42 experiment was repeated with media changes every 4 days, allowing the cells more time to degrade the polyP42; and (2) this same feeding schedule was repeated using the shorter chain polyP17, which would require less processing by the cells. PolyP17 was used at a concentration of 247 μM (representing 4.2 mM Pi equivalents) or 412 μM polyP17 (7.0 mM Pi equivalents) to ensure sufficient Pi was generated. In all cases, the von Kossa and Alizarin red staining were negative in the polyP-treated cultures (Fig. 1D-iii depicts 412 μM polyP17 treatment), although mineralization was maintained in control cultures treated with βGP (Fig. 1D-ii, 3 mM βGP treatment) or Pi (data not shown).

PULSE EXPOSURE OF Saos-2 CELLS TO SHORT CHAIN polyP

To determine whether polyP could have a lasting effect on cell mineralization, Saos-2 cells were treated sequentially with 412 μM polyP17 for 4 days then 3 mM βGP for 3 days. Following the pulse of polyP17, the Saos-2 cells were still able to subsequently metabolize the βGP and form mineral (Fig. 1D). The level of mineral that was formed was less than that observed after 7 days of βGP treatment but was equivalent to the amount of mineral that was formed after 3 days of βGP in 'AA-only' treated cells (Fig. 1D). These data show that there was no carry-over of the effect of polyP on mineralization, suggesting that mineralization inhibition requires continuous polyP presence in the media of Saos-2 cells.

TREATMENT OF MC3T3 CELLS WITH SHORT- AND LONG-CHAIN polyP

Since osteoblast-like cell lines are not all identical, the capacity to utilize polyP could be cell-line dependent. Therefore the mineralization response of Saos-2 cells was contrasted with the response of mouse MC3T3 (which express lower levels of tnALP compared to Saos-2, see supplementary Fig. S1) [Murray et al., 1987; Beck et al., 1998]. Our studies focused on the shorter chain polymer, polyP17, although we repeated these studies using PolyP42 and found little difference between the responses, except where noted.

When MC3T3 cells were cultured in the presence of βGP, deposits became visible during the culture period (light microscopy, Fig. 2A). The deposits appeared to be firmly attached to the cell-matrix layer and were frequently aligned along fibrous components of the matrix. At the end of the 21 days of culture, the deposits were further identified as containing both phosphate (positive von Kossa staining, Fig. 2B) and calcium (positive Alizarin red staining, Fig. 2C). When MC3T3 cells, unlike Saos-2 cells, were cultured in the presence of polyP17, globular clusters could be seen after 14 days in culture (Fig. 2A), however, these clusters were not aligned with fibrous components and were only loosely attached to the cell-matrix layer. Similar clusters were observed under light microscopy with polyP42-treated cells (Fig. 2A, inset). Although fewer clusters were associated with polyP42 than polyP17, this is consistent with the use of a lower concentration of polyP42 polymer chains (119 μM) compared to polyP17 (293 μM) to obtain 5 mM Pi equivalents. Despite the presence of these clusters, von Kossa staining was negative (Fig. 2B). In contrast, when processed with Alizarin red, polyP17-treated cultures exhibited a homogenous bright red stain (Fig. 2C). This stain, however, differed significantly both in pattern and colour from the punctated dark red staining that was observed for βGP- and Pi-induced mineralization. When polyP42-treated wells were stained with Alizarin red, a bright red stain was also initially observed, although it was predominantly removed with subsequent rinsing, leaving a rarefied stained surface (inset, Fig. 2C).

No mineral deposits could be detected using von Kossa staining in MC3T3 cells treated sequentially for 21 days with polyP17, followed by 7 days of βGP or Pi (Fig. 3A). The 21 days treatment with polyP17 followed by a week of continued culture in polyP-free medium resulted in a reduction of the intensity of the red staining (Fig. 3B), although the von Kossa staining remained negative. The Pi concentration in supernatants from MC3T3 cell cultures treated with polyP17 for 21 days was significantly higher than the cells treated with only AA, but lower than the cells treated with βGP (Fig. 3C).

SEM IMAGING AND EDS ANALYSIS OF Saos-2 AND MC3T3 CELL CULTURE MATRIX AFTER MINERALIZATION PERIOD

SEI and BSE images of 21 days βGP-treated MC3T3 cultures identified fine deposits in close association with the fibrous components of the matrix, which generated a strong backscatter signal (Figs. 4A–C). EDS analysis confirmed that the material formed by βGP-treated MC3T3 cells contained ratios in the range of those

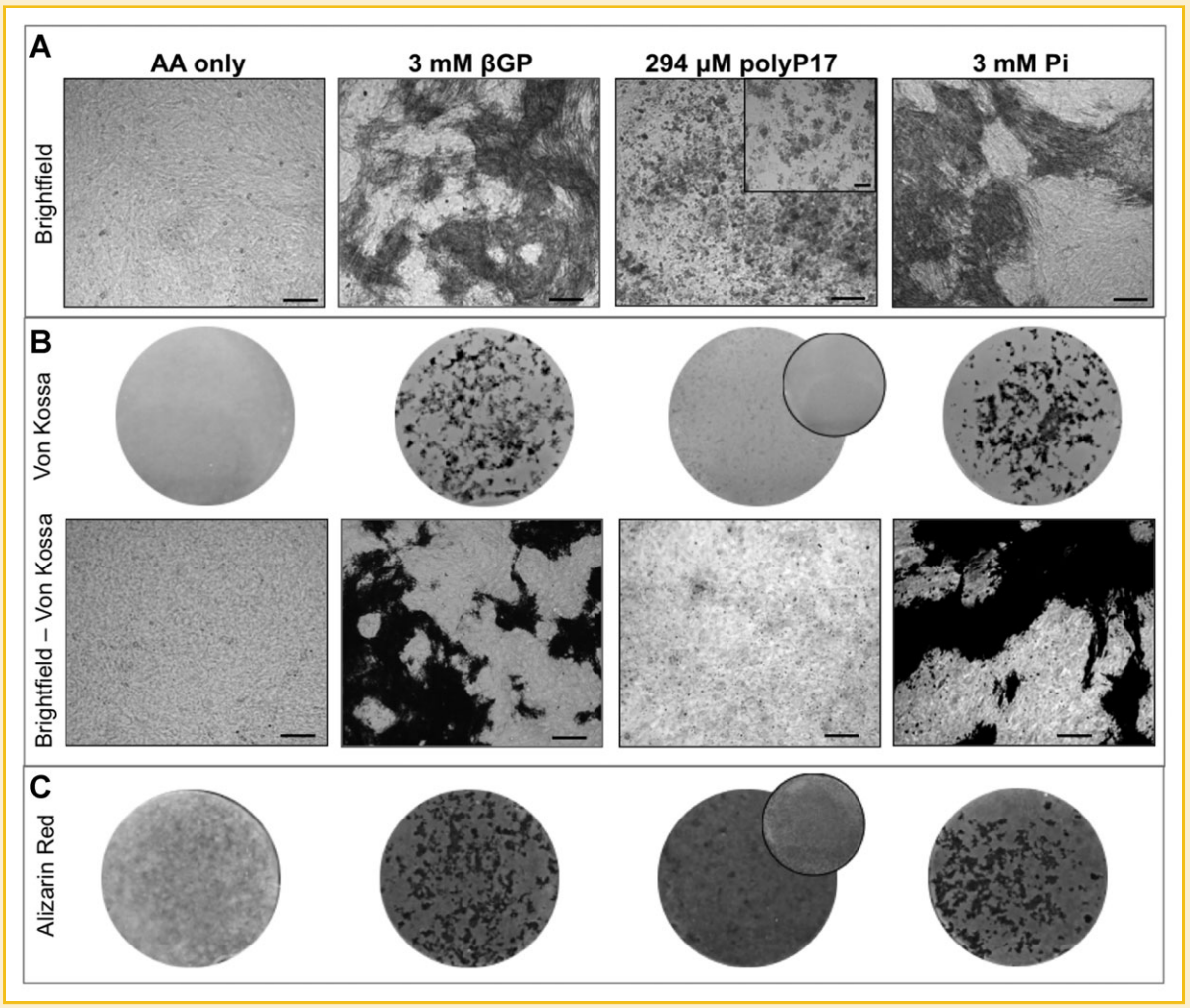

Fig. 2. PolyP cannot be utilized for mineral deposition in 21 d MC3T3 cultures. Mineral deposits were observed under light microscopy (A) in MC3T3 cultures that had been incubated with either βGP or Pi. Clusters of material (likely polyP) were observed after incubation with polyP17, however the morphology did not suggest mineral deposits, and the clusters were localized above the cells, not at the level of the cell matrix, as seen with βGP and Pi treatment. Staining with von Kossa (B) demonstrated the presence of phosphate-containing mineral deposits in cultures treated with either βGP or Pi, however cells treated with polyP17 were negative for von Kossa. Higher magnification images are included to demonstrate that von Kossa staining was negative even at the microscopic level for wells treated with polyP17. Staining with Alizarin red (C) demonstrated a punctate red pattern in βGP or Pi-treated cultures, while polyP17-treated cultures displayed a bright red homogenous staining pattern that differed from the βGP or Pi patterns. The pattern of von Kossa staining of βGP or Pi treated cultures matched the Alizarin red staining, unlike the von Kossa and Alizarin red staining patterns for polyP17 treated cultures which were dissimilar. Similar patterns of staining were seen when the longer chain polymer (polyP42) was used as shown by the inset images, which depict cultures that were treated with 119 μM polyP42 (scale bar = 100 μm).

described for apatite-material [Wergedal and Baylink, 1974; Landis and Glimcher, 1978], with an average Ca:P ratio of 1.43 ± 0.05 (Figs. 5C and F). This was similar to the EDS results obtained with the Saos-2 cells: βGP-treated cultures contained high atomic contrast deposits possessing an apatite-like Ca:P ratio of 1.6 (Fig. 5A). In polyP42-treated Saos-2 cultures, few high atomic contrast areas were identified and no calcium-phosphate deposits were identified by EDS (Fig. 5B). These observations supported the Alizarin red and von Kossa staining results. In contrast to the Saos-2 cultures, imaging of 21 days polyP-treated MC3T3 cultures revealed a large accumulation of material with a high compositional contrast (Figs. 4E–F). Higher magnification of this material showed a distinctively different morphology than the βGP deposits. EDS analysis also revealed differences, specifically the deposits in all polyP17-treated MC-3T3 cultures contained Ca:P ratios less than 1, with an average Ca:P of 0.83 ± 0.07 (Figs. 5D and F). This ratio, indicating the presence of high levels of phosphorus, could result if the phosphorus was present as a condensed polymer chain, suggesting that the electron dense material seen under BSE is likely residual, intact polyP chains chelated with calcium [Mahamid et al., 2011]. Additionally, the detection of higher levels of magnesium in these same electron dense regions provides further support of the presence of residual polyP in these cultures, as polyP can also chelate magnesium. The low magnesium levels in the Saos-2 polyP-treated cultures are consistent with an absence of precipitated polyP at the end of the culture period.

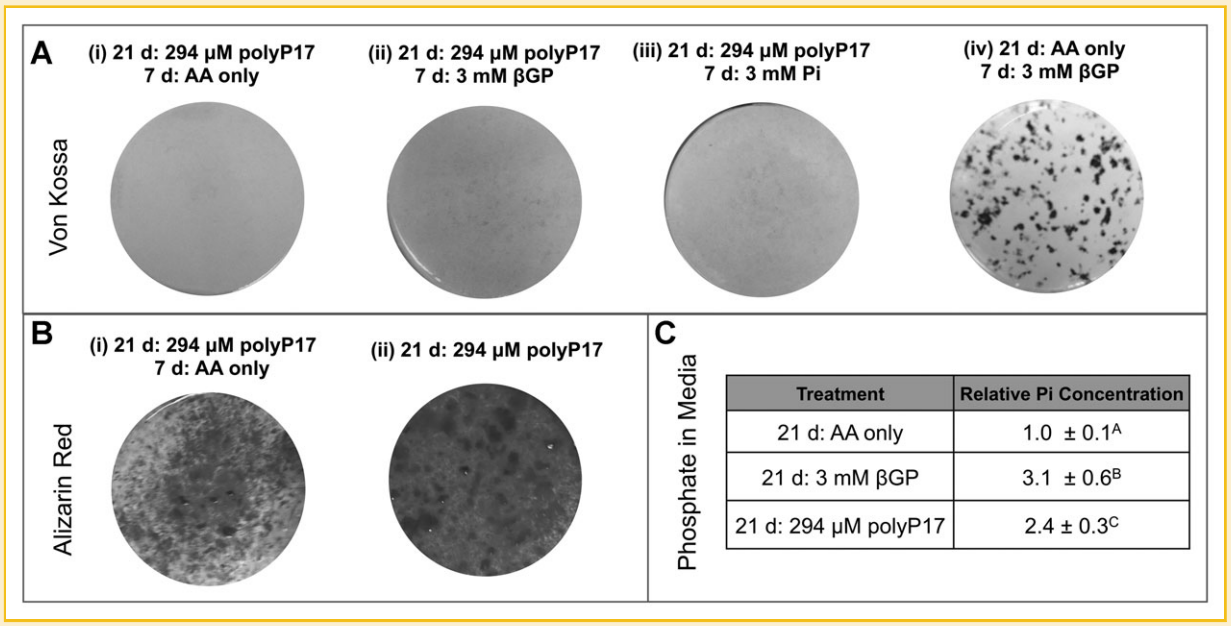

Fig. 3. PolyP is not utilized for mineral deposition in MC3T3 cultures even with sequential treatment of βGP or Pi treatment. Similar to the negative von Kossa staining observed after 21 days of polyP17 supplementation (Fig. 2B), von Kossa staining remained negative despite 7 days of culture in polyP-free media (A-i). This lack of mineral formation was observed even when the cultures were further supplemented with βGP (A-ii) or Pi (A-iii) for 7 days. This is in contrast to the observations for Saos-2 cells, where the mineral inhibition mediated by polyP was transient following βGP supplementation (Fig. 1D-v). Control cultures that were treated for 21 days with AA only were subsequently treated with βGP for 7 days (A-iv) resulting in a strong von Kossa staining, indicating that a 7 days incubation with βGP would be sufficient to generate new mineral deposits in these cultures. The intensity of Alizarin red staining observed after 21 days polyP17 treatment (B-i) was reduced when samples were cultured for an additional 7 days in the presence of polyP-free media (B-ii). This difference in Alizarin red staining was not mirrored by von Kossa, as all polyP-treated wells remained von Kossa negative (A). The supernatents of MC3T3 cells analyzed at the end of a 21 days culture contained different concentrations of orthophosphate (C). Specifically, polyP17-supplemented media contained increased phosphate levels over AA-treated controls, although lower phosphate than cells treated with βGP. Different letters denote a statistical difference at $P < 0.05$.

INFECTION OF MC3T3s WITH A LENTIVIRAL VECTOR FOR tnALP

MC3T3 cells express moderate endogenous levels of tnALP (Fig. S1). To examine whether an increase in tnALP expression enhanced metabolism of polyPs, we overexpressed this enzyme using a lentivirus encoding for tnALP (Fig. 6A). A high expression of the transgene was maintained for at least six passages as determined by positive Fast Blue staining and ALP enzyme activity (Figs. 6B–D).

TREATMENT OF LV-tnALP INFECTED MC3T3s WITH polyP

MC3T3 cells overexpressing tnALP were treated with βGP, Pi or polyP17. The functional significance of this overexpression was demonstrated by the observation that LV-tnALP expressing MC3T3s treated with βGP began to mineralize at least 5 days earlier (by Day 9 in our culture system) compared to control cells (Fig. 6B, as assessed by brightfield imaging). Despite causing earlier mineral deposition, the LV-tnALP treatment did not alter the overall mineral deposition during the 28 days culture period (e.g., pattern of deposition nor amount) (as confirmed by Alizarin red and von Kossa, Fig. 7). The mineralization by polyP-treated cells was unaffected by LV-tnALP overexpression; polyP-treated LV-tnALP cells remained von Kossa negative, while the non-specific homogeneous Alizarin red staining was unaltered.

LONG-TERM TREATMENT OF Saos-2 CELLS WITH polyP

The continuous addition of polyP could lead to a build-up of unprocessed polymer and thus explain the increased Alizarin red staining observed at the end of the MC3T3 culture (up to 28 days). In contrast, routine Saos-2 cultures require only two or three media changes, limiting the opportunity for the build-up of polyP, which may explain the lack of Alizarin red staining in these cultures. To match the protocol used of MC3T3s, we extended the culture period of Saos-2 cells to 21 days, requiring 6 media exchanges. Even at the end of the extended culture of Saos-2 cells with polyP17, there was no microscopic evidence of polyP accumulation and again the polyP-treated wells stained negative for both Alizarin red and von Kossa (Fig. 8). This result suggests that polyP may interact with the extracellular matrix/cell surface of Saos-2 cultures in a manner different from MC3T3 cells, allowing it to be easily removed with successive media changes.

DISCUSSION

Research into the physiological roles of polyP is gaining in popularity. While some interest has focused on the indirect role of intact polyP on the processes of mineralization (including the ability to bind and/or stabilize fibroblast growth factor (FGF)) [Kawazoe et al., 2008], this study focused on the potential *direct* role of polyP as a source of phosphate. As a bioavailable source of phosphate, polyP depolymerisation would be expected to increase the local phosphate concentration and thus ultimately support apatite mineralization. Similar to pyrophosphate, polyPs could have a dichotomous role in

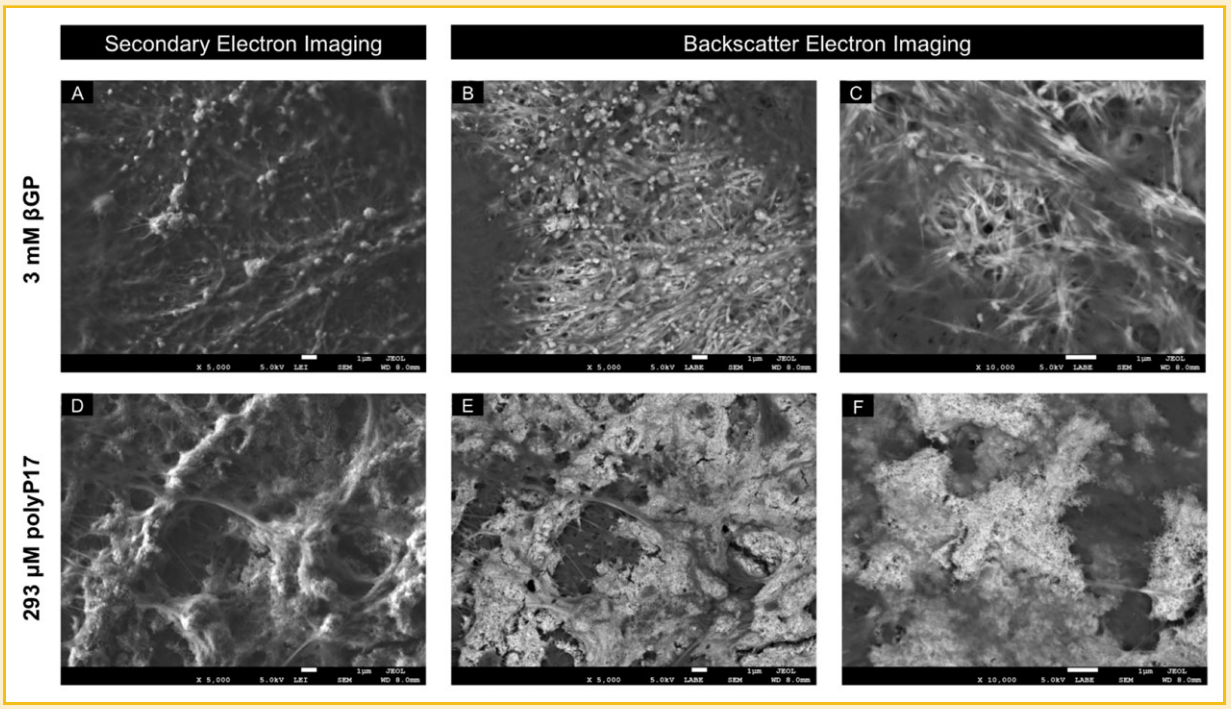

Fig. 4. Electron imaging of 21 days MC3T3 cultures illustrated surface differences due to polyP treatment. Some dissimilarities in the βGP (A) and polyP17 (D) cultures could be observed using SEI, although BSE detection revealed greater differences. BSE of MC3T3 treated with βGP (B, C) showed deposits with a strong backscatter signal associated with and at the level of fibrous material. Cells treated with polyP17 (E, F) showed accumulations of material with a high atomic contrast that were above the cell matrix. Higher magnifications (C, F) revealed distinctly different morphology in the polyP17-treated cultures. Figures A and B are of the same field of view, as are Figures D and E.

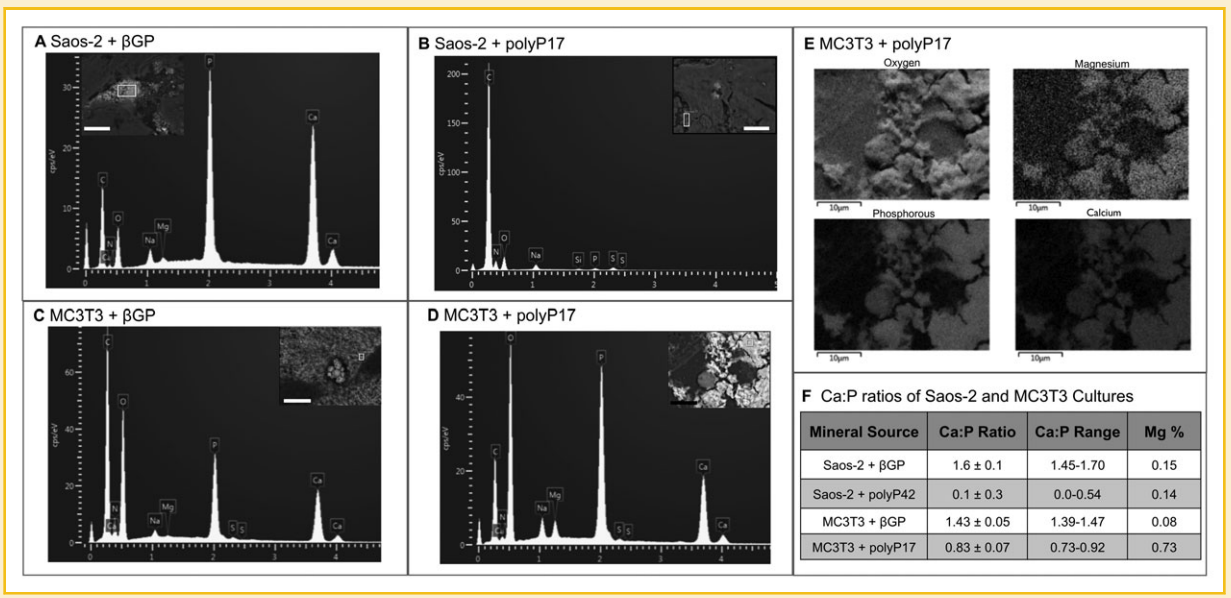

Mineral Source	Ca:P Ratio	Ca:P Range	Mg %
Saos-2 + βGP	1.6 ± 0.1	1.45-1.70	0.15
Saos-2 + polyP42	0.1 ± 0.3	0.0-0.54	0.14
MC3T3 + βGP	1.43 ± 0.05	1.39-1.47	0.08
MC3T3 + polyP17	0.83 ± 0.07	0.73-0.92	0.73

Fig. 5. Electron dispersive spectroscopic elemental maps confirmed differences in surface composition. Representative EDS maps of 4 days Saos-2 and 21 days MC3T3 cultures. Both EDS maps of Saos-2 (A) and MC3T3 (C) cultures treated with βGP demonstrated the presence of calcium-phosphorus deposits on the surface of the cultures. In contrast, EDS maps Saos-2 treated with polyP42 (B) demonstrated a lack of calcium-phosphorus deposits in these cultures. EDS maps of MC3T3 cultures treated with polyP17 (D) revealed the presence of calcium, phosphorus and magnesium on the surface, but not in proportions normally associated with mineral (F). E. Elemental maps of MC3T3 treated with polyP17 (E) culture show that Mg, P, and Ca co-localize.

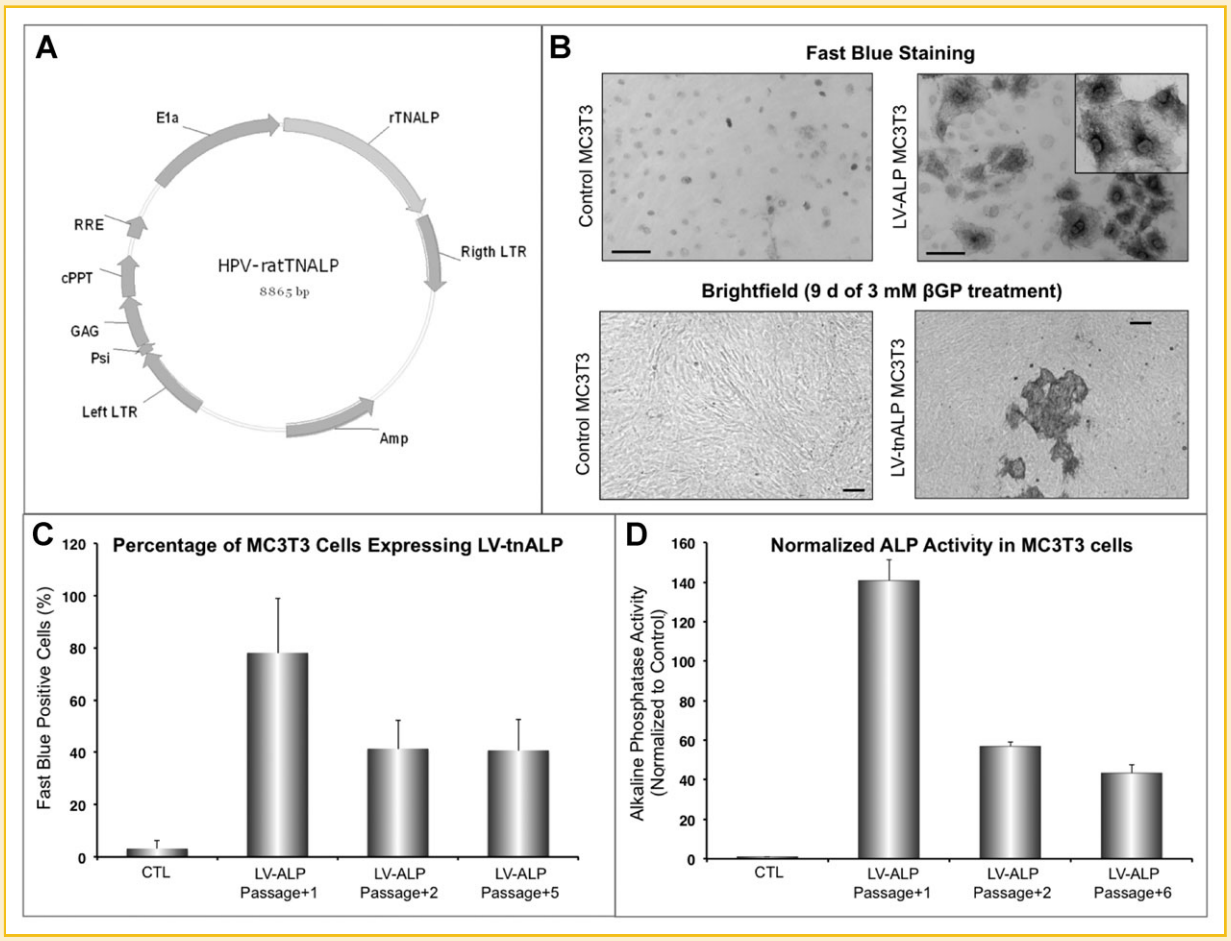

Fig. 6. Alkaline phosphatase lentivirus infection resulted in high enzyme expression and activity in MC3T3 cells. Plasmid map for tnALP vector (A) that was used to create the lentivirus. The map shows that the vector is under the control of EF-1α promoter. Amp: ampicillin resistance gene for bacterial selection; GAG: viral helper gene; LTR: long-term repeats; PSI: RNA packaging signal; cPPT: central polypurine tract; RRE: Reverse responsive element. B. Fast Blue staining for ALP activity (B) demonstrated that MC3T3 cells without LV infection express very little ALP activity, however MC3T3 cells infected with LV-tnALP expressed high levels of ALP (blue stain) even after 5 passages post infection, inset: ALP is expressed throughout the cells and is concentrated in the Golgi (scale bar = 100 μm). Functionally, this overexpression of tnALP resulted in mineralization appearing earlier in 3 mM βGP treated cell cultures (by Day 9, assessed via brightfield microscopy). Quantifying the Fast Blue positive cells (C), almost 80% of the cells expressed LV-tnALP immediately post-infection and 40% of the cells remained positive with extended passages. ALP activity was measured spectrophotometrically (D) and cells retained 45-fold higher ALP activity compared to uninfected controls even with extended passage.

mineralization. When intact, polyPs inhibit mineralization; once completely degraded into Pi they could promote the process. While polyP degradation is likely the result of enzymatic reactions, the phosphatases implicated in polyP processing have not yet been fully identified in mammals. Both intestinal and tnALP have been reported to act as exopolyphosphatases (PPXs) and produce Pi when exposed to polyP [Lorenz and Schröder, 2001; Omelon et al., 2009; Hoac et al., 2013]. Based on these reports, the results of our in vitro study are surprising; no mineralization was found even in the presence of high tnALP activity. This inability to sustain mineral raises two possibilities: incomplete processing of the polymer and/or the implication of other enzymes (discussed below).

Previous studies of ALP-mediated degradation of polyPs were performed under cell-free conditions optimized for ALP activity, specifically simple aqueous alkaline environments with low electrolyte concentrations [Lorenz and Schröder, 2001; Omelon et al., 2009; Hoac et al., 2013]. However, these cell-free, 'biochemically-optimal' assays do not replicate cell culture, nor complex biological environments. Therefore care must be taken when extrapolating the results from such assays to in vitro and physiological systems. In vitro cell culture and in vivo systems contain a variety of additional confounding (albeit physiologically relevant) variables, including high ionic concentration, proteins, cell products and the fact that tnALP is, in principle, bound to cell membranes [Millán, 2006]. All of these factors may influence the kinetics, cleavage products and general feasibility of tnALP-mediated polyP degradation. Despite all these variances, a tacit assumption is made that the degradation kinetics and behavior of polyP in biochemical assays is representative of the actual degradation in complex biological environments. This may be a simplistic assumption, particularly in the case of polyPs, which can complex with proteins and act as chelators of cations [Vandegrift and Evans, 1981]. The possible differences in the

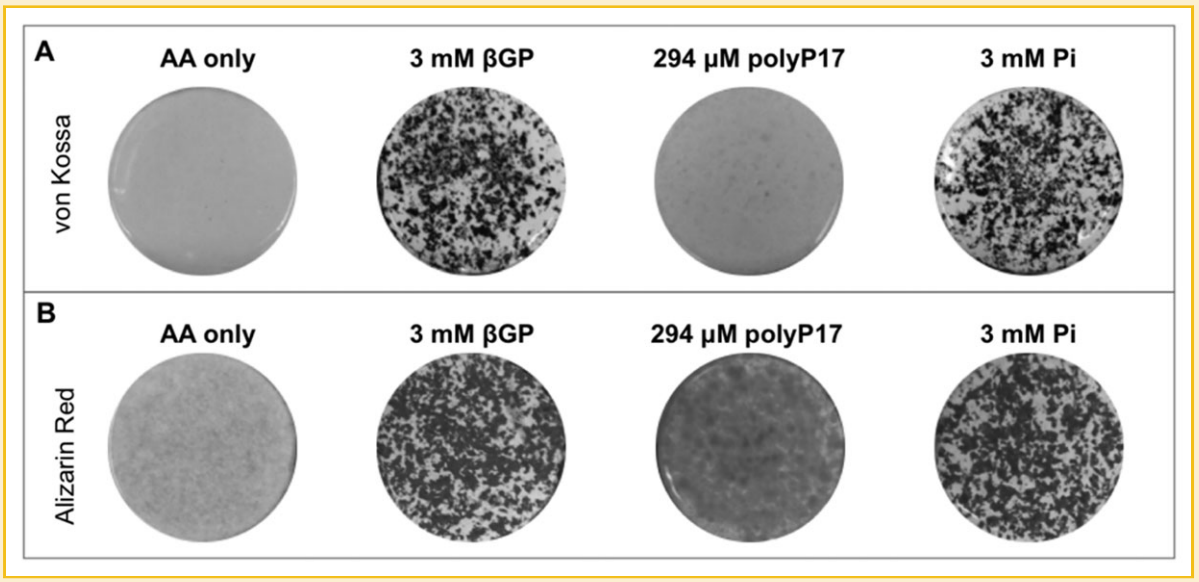

Fig. 7. MC3T3 cells stably overexpressing tnALP did not mineralize in the presence of polyP. Staining with von Kossa (A) demonstrated the presence of phosphate-containing deposits in cells treated for 28 days with either βGP or Pi, however cells treated with polyP17 were negative for von Kossa even at the microscopic level (not shown). The pattern of Alizarin red staining (B) in βGP- or Pi-treated cultures matched the von Kossa staining, however, the Alizarin red and von Kossa staining patterns for polyP17 treated cultures did not match. Similar to uninfected cells (Fig. 2), polyP17-treated cultures displayed a negative von Kossa stain but Alizarin red processing resulted in unique bright red staining that was not representative of the classical punctate staining seen with βGP or Pi in vitro mineralization. The presence of a high expression of tnALP did not alter the lack of mineralization seen in the polyP-treated cultures.

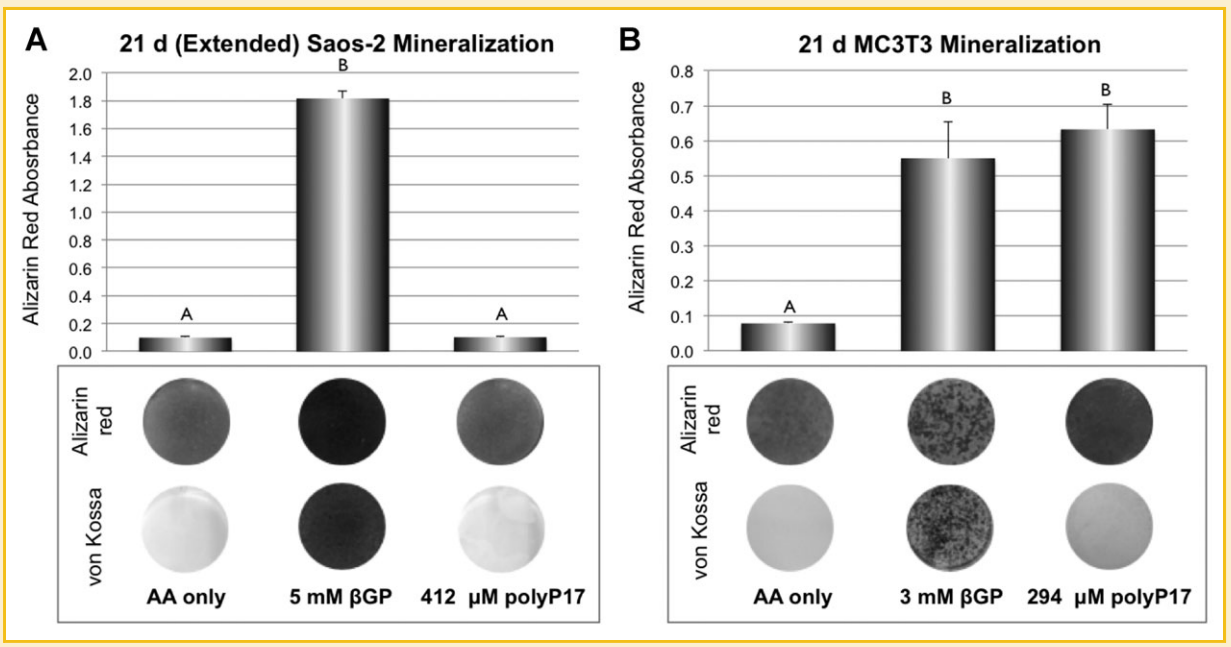

Fig. 8. Mineralization detection using Alizarin red solubilization may lead to inaccurate estimation of mineral deposition in MC3T3 polyP-treated cultures but not Saos-2 cultures. Even after an extended culture period of 21 days (vs 7 days), Saos-2 cells (A) did not utilize polyP17 to form mineral. This was detected using both von Kossa and Alizarin red staining. These staining patterns were accurately reflected when Alizarin red was solubilized for quantification of absorbance. In contrast, when cell cultures of 21 d MC3T3 cells (B) were stained with Alizarin red and then solubilized, the differences in the red staining pattern and stain brightness between βGP- and polyP17-treated cultures was lost upon quantification. The stark differences between Alizarin red staining and von Kossa staining of polyP-treated MC3T3 cells are more predominant when the intact stained cultures are compared. Different letters denote a statistical difference at $P < 0.05$.

kinetics of the enzyme reaction in these two systems would be particularly important for polyP degradation because the continuing presence of even low amounts will act as a mineralization inhibitor [Fleisch et al., 1965; Murray et al., 1987; Beck et al., 1998].

The lack of mineralization seen in our study may actually reflect the persistence of polyPs in the cell culture due to lack of, or incomplete processing, by phosphatases. The large amounts of tnALP present in our Saos-2 and MC3T3 overexpression culture environments implies that the rate of cleavage of extracellular polyP must have been quite slow and/or the enzyme had limited accessibility to terminal phosphates of the chains. Access would be less of a factor in biochemical assays that utilize a free-floating enzyme compared to cell-membrane-bound enzymes (such as tnALP). The gradual loss of polyP following multiple exchanges in polyP-free media (Fig. 3B) suggest either that intact or partially processed polyP can be desorbed from matrix elements over time or eventual metabolism of the polyP could be possible given sufficient time. The increased phosphate concentration in the supernatant of cells treated with polyP17 (Fig. 3C), suggests that exogenous polyP can be cleaved into Pi, but the rate of cleavage is slower than other phosphate precursors such as βGP. The concentration of phosphate in the supernatant of polyP17-treated cells was lower than that of βGP-treated cells, suggesting that even a 4-day incubation period is insufficient to completely cleave all polyP to Pi. This physiological degradation rate will be a significant variable to understand for possible polyP therapies, for example, the time required to reach a critical phosphate concentration to sustain mineralization.

The results of this study lead to a different interpretation than the research of Hoac et al. (2013) where polyP was added to βGP-treated MC3T3 cultures. Based on their biochemical assays, these authors proposed "polyPs competitively saturated TNAP" and that this "potentially interfer[ed] with its ability to hydrolyze...βGP." Our data suggest that tnALP saturation is not the primary mechanism for mineralization inhibition by polyP in vitro (see below). In addition, previous studies by Lorenz and Schröder (2001) have shown that in the presence of excess substrate, the competitive inhibition by polyP is abolished. Other cell culture studies that have shown polyP inhibition of mineralization in the presence of βGP (including ours) use βGP concentrations between 500–1000x higher than polyP. Based on the work by Lorenz and Schröder (2001) in the presence of such a large excess of the βGP substrate, it could be expected that any enzyme competitive effect by polyP would be minimal. There is one additional factor that should be considered when interpreting spectrophotometric (e.g., pNPP) assays that measure the influence of polyPs on ALP activity. Enzyme assays that only measure the chromogenic cleavage product (e.g., *p*-nitrophenol) overlook the physiological cleavage products from the polyP substrate (e.g., Pi). As a result, the activity of the enzyme appears to be decreased, and polyP is thereby interpreted as an enzyme inhibitor (when it might only be acting as a substrate competitor). Therefore, conclusions drawn from this experimental set-up may be inaccurate, and care must be taken when using chromogenic substrates as the exclusive measure of phosphatase activity to determine the inhibitory effect of polyP on phosphate enzymes.

In an attempt to provide more information on the capacity of polyP to directly inhibit ALP under in vitro conditions, we have initiated studies to measure whether the enzyme was still active at the end of the MC3T3 mineralization culture period (see Supplementary Fig. S2). Specifically, ALP activity was measured directly on adherent cells in the plate rather than cell lysates. Our first results (using both pNPP assays and Fast Blue staining) show that ALP remains active in the polyP-treated cultures at levels similar to those in AA only and βGP cultures despite the continuing presence of high concentrations of precipitated polyP17 as demonstrated by the homogenous Alizarin red staining and low Ca:P ratios from EDS. Furthermore, our results with Saos-2 cells (Figs. 1C–V) show that even in conditions that do not require active tnALP to induce mineralization (e.g., the presence of high Pi concentrations [Orimo and Shimada, 2008]), polyP42 treatment still inhibits mineral deposition. Similarly we demonstrate that the addition of free Pi to MC3T3 cultures after polyP17-treatment is also incapable of overcoming the polyP inhibitory effect on mineralization (Fig. 3A). Taken together, we propose that the *persistence* of polyP chains in the local environment of the cells may play a more predominant role in mineralization inhibition than direct tnALP inhibition. This supposition would align well with historical studies that suggested polyP inhibits the initial stages of mineralization, specifically the nucleation process [Fleish and Neuman, 1961; Francis, 1969], possibly by binding (and thus shielding) the first nucleated mineral, and preventing its growth [Amjad, 1987].

A search of polyP literature reveals conflicting observations; in some cases exogenous polyP is reported to stimulate bone mineralization [Fleisch et al., 1966; Hacchou et al., 2007; Usui et al., 2010; Müller et al., 2011; Wang et al., 2012] while other authors report the inhibition of mineralization [Fleisch et al., 1965; Fleisch et al., 1966; Schibler and Fleisch, 1966; Schröder et al., 2000; Hoac et al., 2013]. The discrepancies found in the literature on the function of polyPs may reflect the use of Alizarin red staining as a sole method for quantification; the chemical complexities of the polyP molecule; the differences between cell types and the cell culture techniques themselves. For example, a recent study identified that cell culture media can significantly affect the function of Saos-2 cells; specifically the mineralizing capacity of the cells was compared in αMEM (as used in our study) versus McCoy's media (as used in Müller et al., 2011; Wang et al., 2012). Cells cultured in McCoy's media displayed decreased (a) rates of mineralization, (b) extracellular matrix accumulation, and (c) ALP activity [Lutter et al., 2010]; such changes may cause these cells to resemble MC3T3s in their mineralization behaviour. In other studies, the lack of an appropriate positive control for mineralization (e.g., sufficiently high concentrations of βGP or Pi) complicates interpretation of the data obtained in cell cultures using polyP as a Pi-source, which may lead to inaccurate conclusions. One other component that may be confounding is the style of reporting polyP concentrations. In some studies it is not clear whether the polyP concentration refers to the concentration of the intact polymers, or the concentration of Pi equivalents (see Table I). It is therefore difficult to know whether equivalent polyP concentrations have been used between different studies.

The different types of polyP complexes available and their different dissolution chemistry may further explain some of the divergent results between different studies and also highlight

challenges in the study of polyP as a therapeutic agent. For example, in the absence of any enzymes, sodium polyP compounds are relatively stable in aqueous, neutral environments [Rulliere et al., 2012]. In contrast, the substitution of sodium by certain cations (including Ca^{2+}) may affect the polyP hydrolysis rate. Additionally, the degradation of these cationic complexes during hydrolysis creates an acidic environment that can further accelerate the hydrolytic degradation over time [Watanabe et al., 1975]. A lack of information on the extent of hydrolysis and age of the Ca-polyP complex may further complicate interpretation of results from different studies. In aged solutions, the Ca-polyP polymer may degrade into ortho-, pyro, and tri-phosphate compounds which have lower inhibitory capacities than longer chain polyP [Rulliere et al., 2012].

Given all of these variables, in addition to differences in the chain length of commercially available polyP, it is obvious that standard protocols and in-depth studies are required to understand the mineralization performance of polyP. Ca-polyP complexes should be formed immediately before use so that the polyP is unmodified prior to interaction with cells. In addition, results from our on-going studies suggest that the morphology of Ca-polyP complexes is dependent on the solution in which the complex is formed (see supplementary Fig. S3). We have observed that polyP acquires different morphologies when complexed with Ca^{2+} in the presence of water vs. culture medium. It is not yet clear whether these different morphologies may also reflect differences in hydrolytic stability of the complex or its susceptibility to enzymatic cleavage. It is thus important to be conscious of the exact formulation and method of preparation of polyP reagents and indicate these in the reported experimental protocols since this may have an impact on the interpretation of the results.

The inefficient processing of exogenous polyP in our study should not be interpreted as an overall inability of the cell to process polyPs in general. Broad PPX activity, exclusive from tnALP, has been observed in rat mandibular cell homogenates [Leyhausen et al., 1998], suggesting that phosphate polymers can indeed be metabolized physiologically. At present the particular enzyme(s) that display PPX activity have not yet been isolated and much remains unknown about these enzymes, not just their identity, but also their specific polyP substrate(s), the conditions for optimal activity and the sub-cellular location (e.g., membrane-bound, secreted or cytosolic) [Azevedo and Saiardi, 2014]. The location of the enzyme(s) would be particularly relevant to establish whether the enzymes would be able to process extracellular polyP or only polyP within specific microenvironments.

One other consideration, which has been recently alluded to by David and Quarles (2010), is the distinction between a molecule's in vitro function and its physiological role. The potential therapeutic value of exogenous, synthetic polyP as either an inhibitor or promoter of mineral deposition does not necessarily mean that the physiological function of polyPs will be identical. The chain lengths and chemical environments of the intracellular polyP pool are as yet unknown, and may differ significantly from the synthetic polyP added to cell culture media. Additionally, intracellular polyP may perform indirect functions within the mineralization process, regardless of its ability to act as a direct source of phosphate. Researchers for example, have shown that intact polyP (at concentrations much lower than those used in mineralization studies) can stabilize FGF and serve as a signalling molecule for osteoblasts [Kawazoe et al., 2008], thus suggesting complementary, but indirect mechanisms by which polyP may be involved in mineralization. The potential role of physiological polyP pools in mineral nucleation has yet to be fully determined [Omelon et al., 2009; Mahamid et al., 2011], but their physiological role is not necessarily a prerequisite for synthetic polymers to be prospective therapeutic agents.

The dissimilarity between the von Kossa (negative) and Alizarin red ('positive') staining for polyP-treated MC3T3 cultures suggests that the calcium detected by the Alizarin stain may not be in the form of a traditional calcium-phosphate mineral. The EDS results confirm that MC3T3 cultures contain residual Ca-polyP, providing a mechanism for a positive calcium stain by Alizarin red. Historically, in studies of biological calcification, the presence of red Alizarin staining has been accepted as an indication of calcium phosphate mineral. However, because Alizarin red is a non-specific stain for divalent complexes that are acid-insoluble, it does not specifically stain for calcium mineral nor even calcium itself [Puchtler et al., 1969; Proia and Brinn, 1985]. As our results show, Alizarin red cannot be used as the sole method to evaluate the influence of polyP on mineralization. A variety of recent studies on the effect of polyPs on cell behaviour, including the capacity to induce mineralization [Morrissey, 2012] have relied on Alizarin red to evaluate mineralization. The possibility of an over-estimation of the mineralizing phenotypic changes cannot be excluded in such studies. Furthermore, although an aberrant Alizarin red may be visually detected, direct solubilization of the stain for quantification purposes will miss any anomalous staining (Fig. 8). Finally the possibility of a false positive Alizarin red staining has broad significance for researchers investigating the mineralizing potential of any material that includes divalent cations in its composition, or can chelate divalent cations. The reason for the lack of Alizarin red staining in our polyP-treated Saos-2 cultures remains elusive but may be a function of the extracellular matrix: the organic matrix produced by Saos-2 cells may be unable to anchor polyP, allowing its subsequent elution during media exchanges and staining.

CONCLUSIONS

Our results align with reports that identify intact polyP as an inhibitor of mineralization in the presence of either βGP or Pi. We further demonstrate that under standard, in vitro culture conditions, exogenously added polyPs are unable to act as a complete source of phosphate for initiating mineral deposition. Contrary to what had been proposed in the literature, our results demonstrate that tnALP activity levels are not the limiting factors in this process and rather suggest the kinetics of polyP hydrolysis dominates. The inhibitory influence of exogenous polyP is likely multi-factorial and may involve cellular effects as well as physical interference, although the persistence of intact polyP in these cultures would appear to be a major determinant.

ACKNOWLEDGMENTS

This work was supported by the Canadian Institutes of Health Research (AN) and the Natural Sciences and Engineering Research Council of Canada (AN, SO, FV). MBA is a recipient of a post-doctoral fellowship from the Fonds de Recherche du Québec – Santé. We are thankful to Dr. Candida Parisi (University of Bologna, Italy) for her assistance with Fast Blue staining. PM is supported by the Shriners of North America. FV and SO acknowledge start-up funding from the University of Ottawa. AN and PM are members of Le Réseau de Recherché en Santé Buccodentaire et Osseuse (RSBO) and acknowledge its financial support. AN is a member of the NSERC CREATE program Cellular Dynamics of Macromolecular Complexes (CDMC). We thank JEOL-USA Inc. for their assistance collecting elemental maps.

REFERENCES

Abramov AY, Fraley C, Diao CT, Winkfein R, Colicos MA, Duchen MR, French RJ, Pavlov E. 2007. Targeted polyphosphatase expression alters mitochondrial metabolism and inhibits calcium-dependent cell death. Proc Natl Acad Sci USA 104:18091–18096.

Amjad Z. 1987. The influence of polyphosphates, phosphonates, and poly (carboxylic acids) on the crystal growth of hydroxyapatite. Langmuir 3:1063–1069.

Azevedo C, Saiardi A. 2014. Functions of inorganic polyphosphates in eukaryotic cells: a coat of many colours. Biochem Soc Trans 42:98–102.

Beck GR, Sullivan EC, Moran E, Zerler B. 1998. Relationship between alkaline phosphatase levels, osteopontin expression, and mineralization in differentiating MC3T3-E1 osteoblasts. J Cell Biochem 68:269–280.

David V, Quarles LD. 2010. ASARM mineralization hypothesis: a bridge too far. J Bone Miner Res 25:692–694.

Fleisch H, Schibler D, Maerki J, Frossard I. 1965. Inhibition of aortic calcification by means of pyrophosphate and polyphosphates. Nature 207:1300–1301.

Fleisch H, Straumann F, Schenk R, Bisaz S, Allgower M. 1966. Effect of condensed phosphates on calcification of chick embryo femurs in tissue culture. Am J Physiol 211:821–825.

Fleish H, Neuman WF. 1961. Mechanisms of calcification: role of collagen, polyphosphates, and phosphatase. Am J Physiol 200:1296–1300.

Francis MD. 1969. The inhibition of calcium hydroxyapatite crystal growth by polyphosphonates and polyphosphates. Calcif Tissue Res 3:151–162.

Gray MJ, Wholey W-Y, Wagner NO, Cremers CM, Mueller-Schickert A, Hock NT, Krieger AG, Smith EM, Bender RA, Bardwell JCA, Jakob U. 2014. Polyphosphate Is a Primordial Chaperone. Molecular Cell 53:689–699.

Hacchou Y, Uematsu T, Ueda O, Usui Y, Uematsu S, Takahashi M, Uchihashi T, Kawazoe Y, Shiba T, Kurihara S. 2007. Inorganic polyphosphate: a possible stimulant of bone formation. J Dent Res 86:893–897.

Hoac B, Kiffer-Moreira T, Millán JL, McKee MD. 2013. Polyphosphates inhibit extracellular matrix mineralization in MC3T3-E1 osteoblast cultures. Bone 53:478–486.

Holmström KM, Marina N, Baev AY, Wood NW, Gourine AV, Abramov AY. 2013. Signalling properties of inorganic polyphosphate in the mammalian brain. Nat Comms 4:1362–1369.

Kawazoe Y, Katoh S, Onodera Y, Kohgo T, Shindoh M, Shiba T. 2008. Activation of the FGF signaling pathway and subsequent induction of mesenchymal stem cell differentiation by inorganic polyphosphate. Int J Bio Sci 4:37–47.

Kohn G, Delvaux D, Lakaye B, Servais A-C, Scholer G, Fillet M, Elias B, Derochette J-M, Crommen J, Wins P. 2012. High inorganic triphosphatase activities in bacteria and Mammalian cells: identification of the enzymes involved. PLoS ONE 7:e43879.

Kornberg A, Rao NN, Ault-Riché D. 1999. Inorganic Polyphosphate: a molecule of many functions. Annu Rev Biochem 68:89–125.

Kumble KD, Kornberg A. 1995. Inorganic polyphosphate in mammalian cells and tissues. J Biol Chem 270:5818–5822.

Kumble KD, Kornberg A. 1996. Endopolyphosphatases for long chain inorganic polyphosphate in yeast and mammals. J Biol Chem 271:27146–27151.

Landis WJ, Glimcher MJ. 1978. Electron diffraction and electron probe microanalysis of the mineral phase of bone tissue prepared by anhydrous techniques. J Ultrastruct Mol Struct Res 63:188–223.

Leyhausen G, Lorenz B, Zhu H, Geurtsen W, Bohnensack R, Müller WE, Schröder HC. 1998. Inorganic polyphosphate in human osteoblast-like cells. J Bone Miner Res 13:803–812.

Lorenz B, Schröder HC. 2001. Mammalian intestinal alkaline phosphatase acts as highly active exopolyphosphatase. Biochim Biophys Acta 1547:254–261.

Lutter AH, Hempel U, Wolf-Brandstetter C, Garbe AI, Goettsch C, Hofbauer LC, Jessberger R, Dieter P. 2010. A novel resorption assay for osteoclast functionality based on an osteoblast-derived native extracellular matrix. J Cell Biochem 109:1025–1032.

Mahamid J, Sharir A, Gur D, Zelzer E, Addadi L, Weiner S. 2011. Bone mineralization proceeds through intracellular calcium phosphate loaded vesicles: a cryo-electron microscopy study. J Struct Biol 174:527–535.

Meloan SN, Puchtler H. 1985. Chemical mechanisms of staining methods: von kossa's technique: what von kossa really wrote and a modified reaction for selective demonstration of inorganic phosphates. J Histotechnol 8:11–13.

Millán JL. 2006. Alkaline phosphatases. Purinergic Signal 2:335–341.

Morrissey JH. 2012. Polyphosphate multi-tasks. J Thromb Haemost 10:2313–2314.

Müller F, Mutch NJ, Schenk WA, Smith SA, Esterl L, Spronk HM, Schmidbauer S, Gahl WA, Morrissey JH, Renné T. 2009. Platelet polyphosphates are proinflammatory and procoagulant mediators in vivo. Cell 139:1143–1156.

Müller WEG, Wang X, Diehl-Seifert B, Kropf K, Schlossmacher U, Lieberwirth I, Glasser G, Wiens M, Schröder HC. 2011. Inorganic polymeric phosphate/polyphosphate as an inducer of alkaline phosphatase and a modulator of intracellular Ca^{2+} level in osteoblasts (SaOS-2 cells) in vitro. Acta Biomater 7:2661–2671.

Murray E, Provvedini D, Curran D, Catherwood B, Sussman H, Manolagas S. 1987. Characterization of a human osteoblastic osteosarcoma cell line (SAOS-2) with high bone alkaline phosphatase activity. J Bone Miner Res 2:231–238.

Omelon S, Georgiou J, Henneman ZJ, Wise LM, Sukhu B, Hunt T, Wynnyckyj C, Holmyard D, Bielecki R, Grynpas MD. 2009. Control of vertebrate skeletal mineralization by polyphosphates. Orgel JPRO, editor. PLoS ONE 4:e5634.

Orimo H, Shimada T. 2008. The role of tissue-nonspecific alkaline phosphatase in the phosphate-induced activation of alkaline phosphatase and mineralization in SaOS-2 human osteoblast-like cells. Mol Cell Biochem 315:51–60.

Pavlov E, Aschar-Sobbi R, Campanella M, Turner RJ, Gomez-Garcia MR, Abramov AY. 2010. InOrganic polyphosphate and energy metabolism in mammalian cells. J Biol Chem 285:9420–9428.

Proia AD, Brinn NT. 1985. Identification of calcium oxalate crystals using alizarin red S stain. Arch Pathol Lab Med 109:186–189.

Puchtler H, Meloan SN, Terry MS. 1969. On the history and mechanism of alizarin red S stains. J Histochem Cytochem 17:110–124.

Rulliere C, Perenes L, Senocq D, Dodi A, Marchesseau S. 2012. Heat treatment effect on polyphosphate chain length in aqueous and calcium solutions. Food Chem 134:712–716.

Schibler D, Fleisch H. 1966. Inhibition of skin calcification (calciphylaxis) by polyphosphates. Cell Mol Life Sci 22:367–369.

Schröder HC, Kurz L, Müller W, Lorenz B. 2000. Polyphosphate in bone. Biochemistry (Mosc) 65:296–303.

Smith SA, Mutch NJ, Baskar D, Rohloff P, Docampo R, Morrissey JH. 2006. Polyphosphate modulates blood coagulation and fibrinolysis. Proc Natl Acad Sci USA 103:903–908.

Stanford CM, Jacobson PA, Eanes ED, Lembke LA, Midura RJ. 1995. Rapidly forming apatitic mineral in an osteoblastic cell line (Umr 10601 Bsp). J Biol Chem. 270:9420–9428.

Usui Y, Uematsu T, Uchihashi T, Takahashi M, Takahashi M, Ishizuka M, Doto R, Tanaka H, Komazaki Y, Osawa M, et al. 2010. Inorganic Polyphosphate Induces Osteoblastic Differentiation. J Dent Res 89:504–509.

Van Wazer JR, Campanella DA. 1950. Structure and properties of the condensed phosphates. IV. Complex ion formation in polyphosphate solutions. J Am Chem Soc. 72:655–663.

Vandegrift V, Evans RR. 1981. Polyphosphate binding interactions with bovine serum albumin in protein-polyphosphate precipitates. J Agric Food Chem 29:536–539.

Wang X, Schröder HC, Diehl-Seifert B, Kropf K, Schlossmacher U, Wiens M, Müller WEG. 2012. Dual effect of inorganic polymeric phosphate/polyphosphate on osteoblasts and osteoclasts in vitro. J Tissue Eng Regen Med 7:767–776.

Watanabe M, Sato S, Saito H. 1975. The mechanism of the hydrolysis of condensed phosphates. II. The mechanism of the degradation of long-chain polyphosphates. Bull Chem Soc Jpn 48:896–898.

Wazen RM, Moffatt P, Zalzal SF, Daniel NG, Westerman KA, Nanci A. 2006. Local gene transfer to calcified tissue cells using prolonged infusion of a lentiviral vector. Gene Ther 13:1595–1602.

Wergedal JE, Baylink DJ. 1974. Electron microprobe measurements of bone mineralization rate in vivo. Am J Physiol 226:345–352.

Zakharian E, Thyagarajan B, French RJ, Pavlov E, Rohacs T. 2009. Inorganic polyphosphate modulates TRPM8 channels. PLoS ONE 4:e5404.

SUPPORTING INFORMATION

Additional supporting information may be found in the online version of this article at the publisher's web-site.